

1 **Transfer entropy and cumulant based cost as**
2 **measures of nonlinear causal relationships in space**
3 **plasmas: applications to D_{st}**

Jay R. Johnson

4 Andrews University, Berrien Springs, MI, USA

Simon Wing

5 The Johns Hopkins University, Applied Physics Laboratory, Laurel,

6 Maryland, USA

Enrico Camporeale

7 Center for Mathematics and Computer Science (CWI), Amsterdam, The

8 Netherlands

Jay R. Johnson, Andrews University, Berrien Springs, MI, 49104, USA. (jrj@andrews.edu)

Simon Wing, The Johns Hopkins University, Applied Physics Laboratory, Laurel, Maryland,
20723, USA (simon.wing@jhuapl.edu)

Enrico Camporeale, Center for Mathematics and Computer Science (CWI), Amsterdam, The
Netherlands (e.camporeale@cwi.nl)

9 **Abstract.** It is well known that the magnetospheric response to the so-
10 lar wind is nonlinear. Information theoretical tools such as mutual informa-
11 tion, transfer entropy, and cumulant based analysis are able to characterize
12 the nonlinearities in the system. Using cumulant based cost, we show that
13 nonlinear significance of D_{st} peaks at 3–12 hours lags that can be attributed
14 to VBs , which also exhibit similar behavior. However, the nonlinear signif-
15 icance that peaks at lags 25, 50, and 90 hours can be attributed to internal
16 dynamics, which may be related to the relaxation of the ring current. These
17 peaks are absent in the linear and nonlinear self-significance of VBs . Our
18 analysis with mutual information and transfer entropy show that both meth-
19 ods can establish that there are a strong correlation and transfer of infor-
20 mation from V_{sw} to D_{st} at a time scale that is consistent with that obtained
21 from the cumulant based analysis. However, mutual information also shows
22 that there is a strong correlation in the backward direction, from D_{st} to V_{sw} ,
23 which is counterintuitive. In contrast, transfer entropy shows that there is
24 no or little transfer of information from D_{st} to V_{sw} , as expected because it
25 is the solar wind that drives the magnetosphere, not the other way around.
26 Our case study demonstrates that these information theoretical tools are quite
27 useful for space physics studies because these tools can uncover nonlinear
28 dynamics that cannot be seen with the traditional analyses and models that
29 assume linear relationships.

1. Introduction

30 One of the most practically important concepts in dynamical systems is the notion of
 31 causality. It is particularly useful to organize observational datasets according to causal
 32 relationships in order to identify variables that drive the dynamics. Understanding causal
 33 dependencies can also help to simplify descriptions of highly complex physical processes
 34 because it constrains the coupling functions between the dynamical variables. Analysis
 35 of those coupling functions can lead to simplification of the underlying physical processes
 36 that are most important for driving the system. It is particularly useful from a practi-
 37 cal standpoint to understand causal dependencies in systems involving natural hazards
 38 because monitoring of causal variables is closely linked with warning.

A common method to establish causal dependencies in a data stream of two variables,
 e.g., $[a(t)]$ and $[b(t)]$, is to apply linear correlation studies such as *Strangeway et al.* [2005],
 which showed the relationship between downward Poynting flux and ion outflows. Causal
 relationships are typically identified by considering a time-shifted correlation function

$$\lambda_{ab}(\tau) \triangleq \frac{\langle a(t)b(t+\tau) \rangle - \langle a \rangle \langle b \rangle}{\sqrt{\langle a^2 \rangle - \langle a \rangle^2} \sqrt{\langle b^2 \rangle - \langle b \rangle^2}} \quad (1)$$

39 where $\langle \dots \rangle$ is an ensemble average obtained by drawing samples at a set of measurement
 40 times, $\{t_0, t_1, \dots, t_N\}$. For example, [*Borovsky et al.*, 1998] used such a method to iden-
 41 tify relationships between solar wind variables and plasma sheet variables. The causal
 42 dependency that the plasma sheet responds to changes in the solar wind can be identified
 43 from the time-shift of the peak of the cross correlation indicating a response time. From
 44 this type of analysis it can be found that the plasma sheet generally responds from the

45 tail to the inner magnetosphere consistent with the notion of earthward convection. Such
46 analysis has been particularly useful to help understand plasma sheet transport.

47 However, the procedure of detecting causal relationships based on linear cross-
48 correlation suffers from a number of limitations. First it should be noted that the statisti-
49 cal accuracy of the correlation function is limited by the resolution and length of the data
50 stream. Second, the linear time series analysis ignores nonlinear correlations, which may
51 be important for energy transfer in the magnetospheric system. For example, substorms
52 are believed to involve storage and release of energy in the magnetotail, which is a highly
53 nonlinear response. Similarly, magnetosphere-ionosphere coupling may also be highly non-
54 linear involving the nonlinear development of accelerating potentials along auroral field
55 lines and nonlinear current-voltage relationships. Third, the cross-correlation may not
56 be a particularly clear measure when there are multiple peaks or if there is little or no
57 asymmetry in the forward [i.e., $\lambda_{ab}(\tau)$] and backward directions [i.e., $\lambda_{ba}(\tau) = \lambda_{ab}(-\tau)$].
58 Finally, the cross-correlation does not provide any way to clearly distinguish between two
59 variables that are passively correlated because of a common driver rather than causally
60 related.

61 In the remainder of this paper, we will discuss other methods to identify causal rela-
62 tionships based on entropy based discriminating statistics such as mutual information and
63 transfer entropy. We will also discuss the cumulant-based method. We will illustrate the
64 shortcomings and strengths of the various methods for studying causality with examples
65 from nonlinear dynamics and space physics.

2. Linear vs Nonlinear Dependency

66 It is well known that the magnetosphere responds to variation in the solar wind param-
 67 eters [*Clauer et al.*, 1981; *Baker et al.*, 1983; *Crooker and Gringauz*, 1993; *Papitashvili*
 68 *et al.*, 2000; *Wing and Johnson*, 2015; *Johnson and Wing*, 2015; *Wing et al.*, 2016], and
 69 it has been established that the magnetosphere has a significant linear response to the
 70 solar wind. However, it is also expected that the magnetosphere has a nonlinear response
 71 [*Tsurutani et al.*, 1990; *Vassiliadis et al.*, 1990; *Klimas et al.*, 1998; *Valdivia et al.*, 2013;
 72 *Balikhin et al.*, 2011]. The nonlinear response may driven by internal dynamics rather
 73 than driven externally [*Wing et al.*, 2005; *Johnson and Wing*, 2005]. For example, the
 74 internal dynamics associated with loading and unloading of magnetic energy associated
 75 with storms and substorms is nonlinear [e.g., *Johnson and Wing*, 2014, and references
 76 therein]. Indeed, the data analysis of *Bargatze et al.* [1985] indicated that the dynamical
 77 response of the magnetosphere to solar wind input could not be entirely understood using
 78 linear prediction filters.

Suppose that we consider a set of variables \mathbf{a} and \mathbf{b} which could be vectors of variables measured in time and we would like to measure their dependency. Instead of considering the covariance matrix/correlation function, we consider a more general measure of dependency between an input and output is obtained by considering whether

$$P(\mathbf{a}, \mathbf{b}) \stackrel{?}{=} P(\mathbf{a})\mathbf{P}(\mathbf{b}). \quad (2)$$

79 where $P(\mathbf{a}, \mathbf{b})$ is the joint probability of input \mathbf{a} and output \mathbf{b} while $P(\mathbf{a})$ and $P(\mathbf{b})$ are
 80 the probability of \mathbf{a} and \mathbf{b} respectively. If the relationship holds, then the variables \mathbf{a}
 81 and \mathbf{b} are independent. For all other cases, there is some measure of dependency. In the
 82 case where the system output is completely known given the input, $P(\mathbf{a}, \mathbf{b}) = \mathbf{P}(\mathbf{a})$. The

83 advantage of considering Equation 2 is that it is possible to detect the presence of higher
 84 order nonlinear dependencies between the input and output even in the absence of linear
 85 dependencies [Gershenfeld, 1998].

2.1. Mutual Information and Cumulant based cost

86 Mutual information and cumulant-based cost are two useful measures that quantify
 87 Eq. 2. Mutual information has the advantage that in the limit of Gaussian joint proba-
 88 bility distributions, it may be simply related to the correlation coefficient $C_{ab}(\tau)$ defined
 89 in equation 1 [Li, 1990]. Cumulants have the advantage of good statistics for limited
 90 datasets and noisy systems [Deco and Schürmann, 2000]. Moreover, for high-dimensional
 91 systems it is more efficient to compute moments of the data rather than try to construct
 92 the probability density function.

Correlation studies also only detect linear correlations, so if the feedback involves non-
 linear processes (highly likely in this case) then their usefulness may be seriously limited.
 Alternatively, entropy-based measures such as mutual information [Prichard and Theiler,
 1995; Materassi et al., 2011] and cumulants [Johnson and Wing, 2005] are useful for de-
 tecting linear as well as nonlinear correlations. The mutual information is constructed
 from the probability distribution function of the variables and may be computed using
 an quantization procedure where data is binned such that the samples $[a(t)]$ are assigned
 discrete values $\hat{a} \in \{a_1, a_2, \dots, a_n\}$ of an alphabet \aleph_1 and $[b(t)]$ is assigned discrete values
 $\hat{b} \in \{b_1, b_2, \dots, b_m\}$ of an alphabet \aleph_2 . The *ad hoc* time-shifted mutual entropy

$$\mathcal{M}_{ab}(\tau) \triangleq \sum_{\hat{a} \in \aleph_1, \hat{b} \in \aleph_2} p(\hat{a}(t + \tau), \hat{b}(t)) \log \left(\frac{p(\hat{a}(t + \tau), \hat{b}(t))}{p(\hat{a})p(\hat{b})} \right) \quad (3)$$

93 has been used as an indicator of causality, but suffers from the same problems as time-
 94 shifted cross correlation when it has multiple peaks and long range correlations.

Similarly, examination of time-shifted cumulants could be used as an indicator of causal-
 ity in a nonlinear system. In this case, we can define a discriminating statistic

$$D^C = \sum_{q=1}^{\infty} \sum_{i_1, \dots, i_q \in \Pi_q} K_{1i_2 \dots i_q}^2 \quad (4)$$

where

$$\begin{aligned} K_i &= C_i = \langle z_i \rangle & (4) \\ K_{ij} &= C_{ij} - C_i C_j = \langle z_i z_j \rangle - \langle z_i \rangle \langle z_j \rangle \\ K_{ijk} &= C_{ijk} - C_{ij} C_k - C_{jk} C_i - C_{ik} C_j + 2C_i C_j C_k \\ K_{ijkl} &= C_{ijkl} - C_{ijk} C_l - C_{ijl} C_k - C_{ilk} C_j - C_{ljk} C_i \\ &\quad - C_{ij} C_{kl} - C_{il} C_{kj} - C_{ik} C_{jl} + 2(C_{ij} C_k C_l \\ &\quad + C_{ik} C_j C_l + C_{il} C_j C_k + C_{jk} C_i C_l + C_{jl} C_i C_k \\ &\quad + C_{kl} C_i C_j) - 6C_i C_j C_k C_l \end{aligned}$$

are the cumulants

$$C_{i \dots j} = \int d\mathbf{z} P(\mathbf{z}) z_i \dots z_j \equiv \langle z_i \dots z_j \rangle \quad (5)$$

95 of the joint probability distribution for variables z_1, \dots, z_j .

With only two variables, a and b , defined above, we can consider the cost function

$$D_{a,b}^C(\tau) = D_C(a(t), b(t + \tau)) \quad (6)$$

96 The presence of nonlinear dependence has been identified by comparing the cumulant cost
 97 for a time series with the cumulant based cost of surrogate time series, which are con-
 98 structed to have the same linear correlations as in [*Johnson and Wing, 2005*]). Significance
 99 measures the difference in the discriminating statistic from the mean of the discriminating
 100 statistic of the surrogates in terms of the spread of the surrogates, σ .

101 In Section 3, we will show an application of cumulant based analysis to the distur-
 102 bance storm-time index (D_{st}). In principle, the cross-correlation, mutual information,
 103 and cumulant-based cost should be independent of the selection of measurement points

104 if the system is stationary; therefore, time stationarity can be examined by comparing
 105 these discriminating statistics for groups of measurements drawn from different windows
 106 of time as in [Johnson and Wing, 2005; Wing et al., 2016].

2.2. Transfer entropy

Another method for determining causality is the one-sided transfer entropy [Schreiber, 2000; De Michelis et al., 2011; Materassi et al., 2014; Wing et al., 2016, 2018], which is based upon the conditional mutual information

$$\mathcal{M}_C(x, y|z) \triangleq \sum_{x \in \mathbb{N}_1} \sum_{y \in \mathbb{N}_2} \sum_{z \in \mathbb{N}_3} p(x, y, z) \log \left(\frac{p(x, y, z)p(z)}{p(x, z)p(y, z)} \right) \quad (7)$$

107 The conditional mutual information measures the dependence of two variables, x and y ,
 108 given a conditioner variable, z . If either x or y are dependent on z the mutual information
 109 between x and y is reduced, and this reduction of information provides a method to
 110 eliminate coincidental dependence, or conversely to identify causal dependence.

Transfer entropy considers the conditional mutual information between two variables using the past history of one of the variables as the conditioner.

$$\mathcal{T}_{a \rightarrow b}(\tau) = \sum_{\hat{a} \in \mathbb{N}_1} \sum_{\hat{a}^{(k)} \in \mathbb{N}_1^{(k)}} \sum_{\hat{b} \in \mathbb{N}_2} p(\hat{a}(t + \tau), \hat{a}^{(k)}(t), \hat{b}(t)) \log \left(\frac{p(\hat{a}(t + \tau)|\hat{a}^{(k)}(t), \hat{b}(t))}{p(\hat{a}(t + \tau)|\hat{a}^{(k)}(t))} \right) \quad (8)$$

111 where $\hat{a}^{(k)}(t) = [\hat{a}(t), \hat{a}(t - \Delta), \dots, \hat{a}(t - (k - 1)\Delta)]$. The standard definition of transfer
 112 entropy takes $k = 1$ (no lag), but keeping a higher embedding dimension could in prin-
 113 ciple provide a more precise measure (for example, if a has periodicity a dimension of 2
 114 may provide better prediction of future values of a from its past time series and therefore
 115 lower the transfer entropy. Transfer entropy as a discriminating statistic has the following
 116 advantages. First in the absence of information flow from a to b (i.e., $a(t + \tau)$ has no
 117 additional dependence from $b(t)$ beyond what is known from the past history of $a^{(k)}(t)$)

118 $p(\hat{a}(t + \tau)|\hat{a}^{(k)}(t), \hat{b}(t)) = p(\hat{a}(t + \tau|\hat{a}^{(k)}(t))$ and the transfer entropy vanishes. The transfer
 119 entropy is also highly directional so that $\mathcal{T}_{a \rightarrow b} \neq \mathcal{T}_{b \rightarrow a}$. The advantage can be clearly
 120 seen for dynamical systems where variables are forward differenced and the transfer en-
 121 tropy is clearly one-sided while mutual information and correlation functions can even be
 122 symmetric [Schreiber, 2000]. This measure also accounts for static internal correlations,
 123 which can be used to determine whether two variables are driven by a common driver or
 124 whether the variable b is causally driving the variable a .

125 Both mutual information and transfer entropy require binning of data. As mentioned
 126 in Wing *et al.* [2016], the number of bins (n_b) needs to be chosen properly and there are
 127 some guidelines that can be followed. In general, we would like to maximize the amount
 128 of information. Having too few bins would lump too many points into the same bin,
 129 leading to loss of information. Conversely, having too many bins would leave many bins
 130 with 0 or a few number of points, which also would lead to loss of information. *Sturges*
 131 [1926] proposed that for a normal distribution, optimal $n_b = \log_2(n) + 1$ and bin width
 132 $w = range/n_b$, where n = number of points in the dataset, $range$ = maximum value –
 133 minimum value of the points. In practice, there is usually a range of n_b that would work.

3. Application to space weather: D_{st} analysis

134 D_{st} (disturbance storm time index) is an hourly index that gives a measure of the
 135 strength of the symmetric ring current that, in turn, provides a measure of the dynamics
 136 of geomagnetic storms [Dessler and Parker, 1959]. Because of its global nature, D_{st} is
 137 often used as one of the several indices that represent the state of the magnetosphere.
 138 For example, *Balasis et al.* [2011] used the cumulative square amplitude of D_{st} time series
 139 as a proxy for energy dissipation rate in the magnetosphere and found that it fits well

140 a power law with log-periodic oscillations, which was interpreted as evidence for discrete
141 scale invariance in the D_{st} dynamics.

142 When plasma sheet ions are injected into the Earth inner magnetosphere, they drift
143 westward around the Earth, forming the ring current. Studies have shown that the
144 substorm occurrence rate increases with solar wind velocity (high speed streams) [e.g.,
145 *Kissinger et al.*, 2011; *Newell et al.*, 2016]. An increase in the solar wind electric field,
146 VB_z , can increase the dawn-dusk electric field in the magnetotail, which in turn deter-
147 mines the amount of plasma sheet particles that move to the inner magnetosphere [e.g.,
148 *Friedel et al.*, 2001]. Studies have shown that the electric field, VB_s ($V_{sw} \times$ southward
149 IMF B_z) or VB_z , has a strong effect on the ring current dynamics [*Burton et al.*, 1975;
150 *O'Brien and McPherron*, 2000; *McPherron and O'Brien*, 2001; *Weygand and McPherron*,
151 2006].

152 For the present study, we examine the relationships between solar wind velocity (V_{sw})
153 and VB_s with D_{st} . We use D_{st} records in the period 1974 – 2001 obtained from
154 Kyoto University World Data Center for Geomagnetism ([http://swdcwww.kugi.kyoto-](http://swdcwww.kugi.kyoto-u.ac.jp/index.html)
155 [u.ac.jp/index.html](http://swdcwww.kugi.kyoto-u.ac.jp/index.html)). The corresponding solar wind data are obtained from IMP-8, ACE,
156 WIND, ISEE1, and ISEE3 observations. The ACE SWEPAM and MAG data; and
157 the WIND MAG data are obtained from CDAWeb (<http://cdaweb.gsfc.nasa.gov/>). The
158 WIND 3DP data are obtained from the 3DP team directly. The ISEE1 and ISEE3
159 data are obtained from UCLA (these datasets are also available at NASA NSSDC
160 [<http://nssdc.gsfc.nasa.gov/space/>]). The IMP8 data come directly from the IMP teams.
161 The solar wind is propagated with minimum variance technique [*Weimer et al.*, 2003] to

162 GSM $(X, Y, Z) = (17, 0, 0) R_E$ to produce 1-min files, from which hourly averaged solar
 163 wind parameters are constructed.

3.1. Cumulant based analysis

Section 2.1 presents the method of cumulant based cost. Here, we show an application of cumulant based cost to detect nonlinear dynamics in D_{st} . We consider the forward coupling between a solar wind variable such as VBs and D_{st} , which characterizes the ring current response to the solar wind driver. We therefore consider the nonlinear cross-correlations of the vector

$$\mathbf{c}(t, \tau) = \{VBs(t), D_{st}(t + \tau)\} = \{z_1, z_2\} \quad (9)$$

164 The generalization of cost is based on realizations of $\{z_1, z_2\}$. In this case, each variable
 165 is Gaussianized with unit variance to eliminate static nonlinearities (i.e. higher order
 166 self-correlations in VB_s and D_{st} are eliminated so that the cost measures only cross-
 167 dependence between VBs and D_{st}). This procedure is explained in the next paragraph.

168 The distribution of D_{st} and VBs are generally non-Gaussian. As such, the raw dis-
 169 tributions (e.g., distribution of values of D_{st}) may have nonzero higher-order cumulants
 170 (e.g., they can have a skew and kurtosis). This property makes it more difficult to in-
 171 terpret whether the higher order cumulants in the time evolution arise from the overall
 172 shape of the distribution of data points or from the time-ordering of the data. To elim-
 173 inate the inherent nonzero cumulants in the overall distribution of data, we construct a
 174 rank-ordered map from the original dataset to a proxy dataset of the same length drawn
 175 from a Gaussian distribution [*Kennel and Isabelle, 1992; Schreiber and Schmitz, 1996;*
 176 *Deco and Schürmann, 2000*]. The distribution of the proxy dataset ensures that all cu-

177 mulants of the distribution beyond second order should in principle vanish. However, the
 178 time-ordering of the data can still lead to nonzero cumulants, because the joint probability
 179 distribution of $D_{st}(t+\tau)$ and $D_{st}(t)$ may be non-Gaussian even if the distribution of D_{st} is
 180 Gaussian. Moreover, it is simple to construct surrogate data from the Gaussianized data
 181 that shares the same autocorrelation by using the same power spectrum, but randomly
 182 shifting the phases of the Fourier coefficients. The surrogate data therefore has the same
 183 autocorrelation as the original data. Any deviation from the linear statistic is apparent
 184 from comparison with the surrogate data, and we interpret these deviations as evidence
 185 of nonlinear dependence because we have falsified the hypothesis that the data can be
 186 adequately described by linear statistics. This method has been successfully employed in
 187 *Johnson and Wing* [2005] where K_p record was analyzed with mutual information and
 188 cumulants.

189 In Figure 1 we plot the significance obtained from the year 1999 as a function of time
 190 delay, τ . Significance extracted from $\{VBs(t), D_{st}(t + \tau)\}$ and $\{VBs(t), VBs(t + \tau)\}$
 191 for 1999 are plotted in panels (a) and (b), respectively. It should be noted that there
 192 is a strong linear response at around 3 hour time delay. As shown in Figure 1a, there
 193 is a clear nonlinear response with peaking around 3–10, 25, 50 and 90 hours lasting for
 194 approximately 1 week. In contrast, in Figure 1b, the nonlinearity only has one broad peak
 195 around 3 – 12 hours in the self-significance for VBs , suggesting that the nonlinear and
 196 linear peaks at $\tau = 3$ –12 hours in in Figure 1a i may be associated with VBs . We will
 197 revisit the solar wind causal relationship with D_{st} using transfer entropy in Section 3.2.

198 The absence of the nonlinear peaks at $\tau = 25, 50,$ and 90 hours in the self-significance
 199 for VBs (Figure 1b) suggest that these nonlinearities in $\{VBs(t), D_{st}(t+\tau)\}$ are related to

200 internal magnetospheric dynamics. As the D_{st} index is thought to reflect storm activity,
201 it is reasonable that nonlinear significance would decay on the order of 1 week as storms
202 commonly last around that time. The strong nonlinear responses at $\tau = 25, 50,$ and 90
203 hours are likely related to multiple modes of relaxation of the ring current following the
204 commencement of storms. It should also be noted that other nonlinearities detected by
205 even higher order cumulants may also be present; however, the calculation demonstrates
206 the nonlinear nature of the underlying dynamics.

207 A common scenario for storm-ring current interaction is the following. A storm com-
208 presses the magnetosphere, intensifies the magnetic field in the magnetosphere, and injects
209 energetic particles into the ring current region. The ring current intensifies during the
210 main phase of the storm, which can last ~ 6 hours [*Weygand and McPherron, 2006*].
211 Once the injection stops, the ring current begins to decay and the storm enters the re-
212 covery phase. Conservation of magnetic moment implies that anisotropies develop in the
213 ring current and plasma sheet. Anisotropy drives the ring current plasma unstable to ion
214 cyclotron waves. The ion cyclotron waves scatter energetic ions into the loss cone so that
215 they are lost from the ring current. Nonlinear interaction between waves and particles
216 keeps the plasma near marginal instability with a steady loss of energetic particles due
217 to wave-particle scattering. Other loss mechanisms include charge exchange, coulomb
218 scattering, and convective of ions to the front of the magnetopause. The ring current
219 decay can have two stages [*Kozyra et al., 2002*]. In the first stage, the ring current decays
220 rapidly and the loss mechanisms can be attributed to convective out flow, pitch-angle
221 scattering in the ring current, and O^+ charge exchange [e.g., *Weygand and McPherron,*
222 *2006; Hamilton et al., 1988*]. The second stage may typically begin about one day from

223 the commencement of the storm (see, for example, Figure 7 of *Kozyra et al.* [2002]). In
 224 the second stage, the decay rate is slower and is attributed mainly to H^+ charge exchange
 225 [*Hamilton et al.*, 1988] and can take several days to deplete the ring current to the baseline
 226 level [*Smith et al.*, 1976]. We can speculate that the multiple nonlinear response lag times
 227 that are detected with the cumulant-based approach are likely the relaxation of the ring
 228 current due to complex interplay of multiple loss processes.

3.2. Transfer entropy

229 As mentioned in Section 2.2, transfer entropy gives a measure of how much information
 230 is transferred from one variable to another. We have applied transfer entropy and mutual
 231 information to the relationship between the V_{sw} and D_{st} for the period 1974 – 2001. The
 232 result is shown in Figure 2. Note that the mutual information measure suggests strong
 233 correlations between prior values of D_{st} and V_{sw} . This finding suggests that D_{st} could be
 234 a driver of V_{sw} , which is counterintuitive. On the other hand, the transfer entropy clearly
 235 shows that this information transfer in the backward direction ($D_{st} \rightarrow V_{sw}$) does not rise
 236 above the noise level (the horizontal blue lines indicate mean and standard deviation of
 237 100 surrogate data sets where the data was randomly reordered.) This result is expected
 238 because it is the solar wind that drives the magnetosphere, not the other way around.
 239 The transfer of information from V_{sw} to D_{st} peaks at $\tau = 8 - 11$ hours. The cumulant
 240 based analysis in Section 3.1 shows that the response of D_{st} to VBs has similar time scale.
 241 This time scale is consistent with the 4 to 15 hours transport time for the solar wind to
 242 reach the midnight and noon regions of the geosynchronous orbit, respectively, from the
 243 dayside magnetopause [*Borovsky et al.*, 1998]. The analysis presented here illustrates the
 244 power of the transfer entropy for accessing causality.

4. Summary

245 We recently used mutual information, transfer entropy, and conditional mutual infor-
246 mation to discover the solar wind drivers of the outer radiation belt electrons [*Wing et al.*,
247 2016]. Because V_{sw} anticorrelates with solar wind density (n_{sw}), it is hard to isolate the
248 effects of V_{sw} on radiation belt electrons, given n_{sw} and vice versa. However, using condi-
249 tional mutual information, we were able to determine the information transfer from n_{sw}
250 or any other solar wind parameters to radiation belt electrons, given V_{sw} (or any other
251 solar wind parameters). We also showed that the triangle distribution in the radiation
252 belt electron vs. solar wind velocity plot [*Reeves et al.*, 2011] can be understood better
253 when we consider that V_{sw} and n_{sw} transfer information to radiation belt electrons with
254 2 days and 0 day (< 24 hr) lags, respectively. Also recently, we used transfer entropy to
255 better understand the causal parameters in the solar cycle and their response lag times
256 [*Wing et al.*, 2018].

257 As a follow up to *Wing et al.* [2016, 2018], the present study demonstrates further how
258 information theoretical tools can be useful for space physics and space weather studies.
259 Cumulant based analysis can be used to distinguish internal vs. external driving of the
260 system. Both mutual information and transfer entropy give a measure of shared infor-
261 mation between two variables (or vectors). However, unlike mutual information, transfer
262 entropy is highly directional. To illustrate, we apply mutual information, transfer entropy,
263 and cumulant based analysis to investigate the dynamics of D_{st} index.

264 Our analysis with mutual information and transfer entropy indicates that there are
265 strong linear and nonlinear correlations and transfer of information, respectively, in the
266 forward direction between V_{sw} and D_{st} ($V_{sw} \rightarrow D_{st}$). However, mutual information indi-

267 cates that there is also a strong correlation in the backward direction ($D_{st} \rightarrow V_{sw}$), which
268 is puzzling and counterintuitive. In contrast, the transfer entropy indicates that there is
269 no information transfer in the backward direction ($D_{st} \rightarrow V_{sw}$), as expected because it is
270 the solar wind that drives the magnetosphere, not the other way around. The transfer of
271 information from V_{sw} to D_{st} peaks at $\tau = 8 - 11$ hours.

272 Using the cumulant-based significance, we have established that the underlying dynam-
273 ics of D_{st} is in general nonlinear exhibiting a quasiperiodicity which is detectable only if
274 nonlinear correlations are taken into account. The strong nonlinear responses of D_{st} to
275 VBs at $\tau = 25, 50,$ and 90 hours are likely related to multiple modes of relaxation of the
276 ring current from multiple loss mechanisms following the commencement of storms. It is,
277 of course, possible that these nonlinearities are caused by solar wind drivers other than
278 VBs . However, the timing of these nonlinearities would put them well in the recovery
279 phase of a storm and previous studies suggested that the ring current decays in the recov-
280 ery phase are strongly influenced by VBs [Burton *et al.*, 1975; O'Brien and McPherron,
281 2000; McPherron and O'Brien, 2001]. The nonlinearities at $\tau = 3 - 12$ hours are not
282 caused by internal dynamics but rather by the solar wind driver, which is similar with
283 the time scale for the solar wind transport time from the dayside magnetopause to the
284 inner magnetosphere. This time scale is consistent with the time scale for the information
285 transfer from the solar wind to D_{st} obtained from transfer entropy analysis.

286 Although linear models are useful, our results indicate that these models have to be
287 used with cautions because solar wind – magnetosphere system is inherently nonlinear.
288 Hence, nonlinearities generally need to be taken into account in order to describe the
289 system accurately. Local-linear models (which include slow evolution of parameters) may

290 be able to handle some nonlinearities, but it is expected that these local-linear models
291 would have difficulties if the dynamics suddenly and rapidly change.

292 **Acknowledgments.** All the derived data products in this paper are available
293 upon request by email (simon.wing@jhuapl.edu). Simon Wing acknowledges sup-
294 port from JHU/APL Janney Fellowship, NSF Grant AGS-1058456, and NASA Grants
295 (NNX13AE12G, NNX15AJ01G, NNX16AR10G, and NNX16AQ87G). Jay R. Johnson ac-
296 knowledges support from NASA Grants (NNH11AR07I, NNX14AM27G, NNH14AY20I,
297 NNX16AC39G), NSF Grants (ATM0902730, AGS-1203299, AGS-1405225), and DOE
298 contract DE-AC02-09CH11466. E. Camporeale is partially funded by the NWO-Vidi
299 grant No. 639.072.716. We thank James M. Weygand for the solar wind data processing.
300 The raw solar wind data from ACE, Wind, ISEE1 and ISEE3 were obtained from NASA
301 CDAW and NSSDC.

References

- 302 Baker, D. N., R. D. Zwickl, S. J. Bame, E. W. Hones, B. T. Tsurutani, E. J. Smith, and
303 S.-I. Akasofu (1983), An isee 3 high time resolution study of interplanetary parameter
304 correlations with magnetospheric activity, *Journal of Geophysical Research*, 88(A8),
305 6230, doi:10.1029/ja088ia08p06230.
- 306 Balasis, G., C. Papadimitriou, I. A. Daglis, A. Anastasiadis, L. Athanasopoulou, and
307 K. Eftaxias (2011), Signatures of discrete scale invariance in dst time series, *Geophysical*
308 *Research Letters*, 38(13).
- 309 Balikhin, M. A., R. J. Boynton, S. N. Walker, J. E. Borovsky, S. A. Billings, and H. L. Wei
310 (2011), Using the narmax approach to model the evolution of energetic electrons fluxes

- 311 at geostationary orbit, *Geophys. Res. Lett.*, , 38, L18105, doi:10.1029/2011GL048980.
- 312 Bargatze, L. F., D. N. Baker, E. W. Hones, and R. L. McPherron (1985), Magnetospheric
313 impulse response for many levels of geomagnetic activity, *J. Geophys. Res.*, 90, 6387–
314 6394.
- 315 Borovsky, J. E., M. F. Thomsen, and R. C. Elphic (1998), The driving of the plasma
316 sheet by the solar wind, *J. Geophys. Res.*, 103, 17,617–17,640, doi:10.1029/97JA02986.
- 317 Burton, R. K., R. L. McPherron, and C. T. Russell (1975), An empirical relationship
318 between interplanetary conditions and Dst, *J. Geophys. Res.*, 80, 4204–4214.
- 319 Clauer, C. R., R. L. McPherron, C. Searls, and M. G. Kivelson (1981), Solar wind control
320 of auroral zone geomagnetic activity, *Geophysical Research Letters*, 8(8), 915–918, doi:
321 10.1029/gl008i008p00915.
- 322 Crooker, N. U., and K. I. Gringauz (1993), On the low correlation between long-term
323 averages of solar wind speed and geomagnetic activity after 1976, *Journal of Geophysical*
324 *Research*, 98(A1), 59, doi:10.1029/92ja01978.
- 325 De Michelis, P., G. Consolini, M. Materassi, and R. Tozzi (2011), An information theory
326 approach to the storm-substorm relationship, *Journal of Geophysical Research: Space*
327 *Physics*, 116(A8).
- 328 Deco, G., and B. Schürmann (2000), *Information Dynamics*, Springer.
- 329 Dessler, A. J., and E. N. Parker (1959), Hydromagnetic theory of magnetic storms, *J.*
330 *Geophys. Res.*, 64(2239-2259).
- 331 Friedel, R. H. W., H. Korth, M. G. Henderson, M. F. Thomsen, and J. D. Scudder (2001),
332 Plasma sheet access to the inner magnetosphere, *Journal of Geophysical Research: Space*
333 *Physics*, 106(A4), 5845–5858, doi:10.1029/2000ja003011.

- 334 Gershenfeld, N. (1998), *The Nature of Mathematical Modeling*, Cambridge University
335 Press, Cambridge, chapter.
- 336 Hamilton, D., G. Gloeckler, F. Ipavich, W. Stüdemann, B. Wilken, and G. Kremser (1988),
337 Ring current development during the great geomagnetic storm of february 1986, *Journal*
338 *of Geophysical Research: Space Physics*, *93*(A12), 14,343–14,355.
- 339 Johnson, J. R., and S. Wing (2005), A solar cycle dependence of nonlinearity in magneto-
340 spheric activity, *Journal of Geophysical Research*, *110*(A4), doi:10.1029/2004ja010638.
- 341 Johnson, J. R., and S. Wing (2014), External versus internal triggering of substorms:
342 An information-theoretical approach, *Geophysical Research Letters*, *41*(16), 5748?5754,
343 doi:10.1002/2014gl060928.
- 344 Johnson, J. R., and S. Wing (2015), The dependence of the strength and thickness of
345 field-aligned currents on solar wind and ionospheric parameters, *Journal of Geophysical*
346 *Research: Space Physics*, *120*(5), 3987?4008, doi:10.1002/2014ja020312.
- 347 Kennel, M. B., and S. Isabelle (1992), Method to distinguish possible chaos from colored
348 noise and to determine embedding parameters, *Physical Review A*, *46*, 3111.
- 349 Kissinger, J., R. L. McPherron, T.-S. Hsu, and V. Angelopoulos (2011), Steady magne-
350 tospheric convection and stream interfaces: Relationship over a solar cycle, *Journal of*
351 *Geophysical Research: Space Physics*, *116*(A5), n/a?n/a, doi:10.1029/2010ja015763.
- 352 Klimas, A. J., D. Vassiliadis, and D. N. Baker (1998), Dst index prediction using data-
353 derived analogues of the magnetospheric dynamics, *J. Geophys. Res.*, *103*, 20,435–
354 20,448.
- 355 Kozyra, J., M. Liemohn, C. Clauer, A. Ridley, M. Thomsen, J. Borovsky, J. Roeder,
356 V. Jordanova, and W. Gonzalez (2002), Multistep dst development and ring current

- 357 composition changes during the 4–6 june 1991 magnetic storm, *Journal of Geophysical*
358 *Research: Space Physics*, 107(A8).
- 359 Li, W. (1990), Mutual information functions versus correlation functions, *J. Stat. Phys.*,
360 60, 823.
- 361 Materassi, M., L. Ciruolo, G. Consolini, and N. Smith (2011), Predictive space weather:
362 An information theory approach, *Advances in Space Research*, 47, 877–885, doi:
363 10.1016/j.asr.2010.10.026.
- 364 Materassi, M., G. Consolini, N. Smith, and R. De Marco (2014), Information theory
365 analysis of cascading process in a synthetic model of fluid turbulence, *Entropy*, 16(3),
366 1272–1286.
- 367 McPherron, R. L., and P. O’Brien (2001), Predicting geomagnetic activity: The dst index,
368 *Space Weather*, pp. 339–345.
- 369 Newell, P., K. Liou, J. Gjerloev, T. Sotirelis, S. Wing, and E. Mitchell (2016), Substorm
370 probabilities are best predicted from solar wind speed, *Journal of Atmospheric and*
371 *Solar-Terrestrial Physics*, 146, 28–37, doi:10.1016/j.jastp.2016.04.019.
- 372 O’Brien, T. P., and R. L. McPherron (2000), An empirical phase space analysis of ring
373 current dynamics: Solar wind control of injection and decay, *J. Geophys. Res.*, 105,
374 7707–7720.
- 375 Papitashvili, V. O., N. E. Papitashvili, and J. H. King (2000), Solar cycle effects in
376 planetary geomagnetic activity: Analysis of 36-year long omni dataset, *Geophysical*
377 *Research Letters*, 27(17), 2797–2800, doi:10.1029/2000gl000064.
- 378 Prichard, D., and J. Theiler (1995), Generalized redundancies for time series analysis,
379 *Physica D: Nonlinear Phenomena*, 84(3–4), 476 – 493, doi:10.1016/0167-2789(95)00041-

2.

380

381 Reeves, G. D., S. K. Morley, R. H. W. Friedel, M. G. Henderson, T. E. Cayton, G. Cun-
382 ningham, J. B. Blake, R. A. Christensen, and D. Thomsen (2011), On the relation-
383 ship between relativistic electron flux and solar wind velocity: Paulikas and Blake
384 revisited, *Journal of Geophysical Research: Space Physics*, *116*(A2), n/a?n/a, doi:
385 10.1029/2010ja015735.

386 Schreiber, T. (2000), Measuring information transfer, *Phys. Rev. Lett.*, *85*, 461–464, doi:
387 10.1103/PhysRevLett.85.461.

388 Schreiber, T., and A. Schmitz (1996), Improved surrogate data for nonlinearity tests,
389 *Phys. Rev. Lett.*, *77*, 635–639.

390 Smith, P. H., R. A. Hoffman, and T. A. Fritz (1976), Ring current proton decay by charge
391 exchange, *J. Geophys. Res.*, *81*, 2701–2708, doi:10.1029/JA081i016p02701.

392 Strangeway, R., J. R. E. Ergun, Y.-J. Su, C. W. Carlson, and R. C. Elphic (2005),
393 Factors controlling ionospheric outflows as observed at intermediate altitudes, *Journal*
394 *of Geophysical Research*, *110*(A3), doi:10.1029/2004ja010829.

395 Sturges, H. A. (1926), The choice of class interval, *J. Am. Stat. Assoc.*, *21*, 65–66, doi:
396 10.1080/01621459.1926.10502161.

397 Tsurutani, B. T., M. Sugiura, T. Iyemori, B. E. Goldstein, W. D. Gonzalez, S. I. Akasofu,
398 and E. J. Smith (1990), The nonlinear response of ae to the imf bs driver: A spectral
399 break at 5 hours, *Geophysical Research Letters*, *17*(3), 279–282.

400 Valdivia, J. A., J. Rogan, V. Muñoz, B. A. Toledo, and M. Stepanova (2013), The
401 magnetosphere as a complex system, *Advances in Space Research*, *51*, 1934–1941, doi:
402 10.1016/j.asr.2012.04.004.

- 403 Vassiliadis, D. V., A. S. Sharma, T. E. Eastman, and K. Papadopoulos (1990), Low-
404 dimensional chaos in magnetospheric activity from AE time series, *Geophys. Res. Lett.*,
405 *17*, 1841–1844.
- 406 Weimer, D. R., D. M. Ober, N. C. Maynard, M. R. Collier, D. J. McComas, N. F. Ness,
407 C. W. Smith, and J. Watermann (2003), Predicting interplanetary magnetic field (imf)
408 propagation delay times using the minimum variance technique, *Journal of Geophysical*
409 *Research*, *108*(A1), doi:10.1029/2002ja009405.
- 410 Weygand, J. M., and R. L. McPherron (2006), Dependence of ring current asymmetry
411 on storm phase, *Journal of Geophysical Research (Space Physics)*, *111*, A11221, doi:
412 10.1029/2006JA011808.
- 413 Wing, S., and J. R. Johnson (2015), Theory and observations of upward field-aligned
414 currents at the magnetopause boundary layer, *Geophysical Research Letters*, *42*(21),
415 9149?9155, doi:10.1002/2015gl065464.
- 416 Wing, S., J. R. Johnson, J. Jen, C.-I. Meng, D. G. Sibeck, K. Bechtold, J. Freeman,
417 K. Costello, M. Balikhin, and K. Takahashi (2005), Kp forecast models, *Journal of*
418 *Geophysical Research*, *110*(A4), doi:10.1029/2004ja010500.
- 419 Wing, S., J. R. Johnson, E. Camporeale, and G. D. Reeves (2016), Information theoret-
420 ical approach to discovering solar wind drivers of the outer radiation belt, *Journal of*
421 *Geophysical Research: Space Physics*, doi:10.1002/2016ja022711.
- 422 Wing, S., J. R. Johnson, and A. Vourlidas (2018), Information theoretic approach to
423 discovering causalities in the solar cycle, *Astrophys. J.*, , *854*, 85, doi:10.3847/1538-
424 4357/aaa8e7.

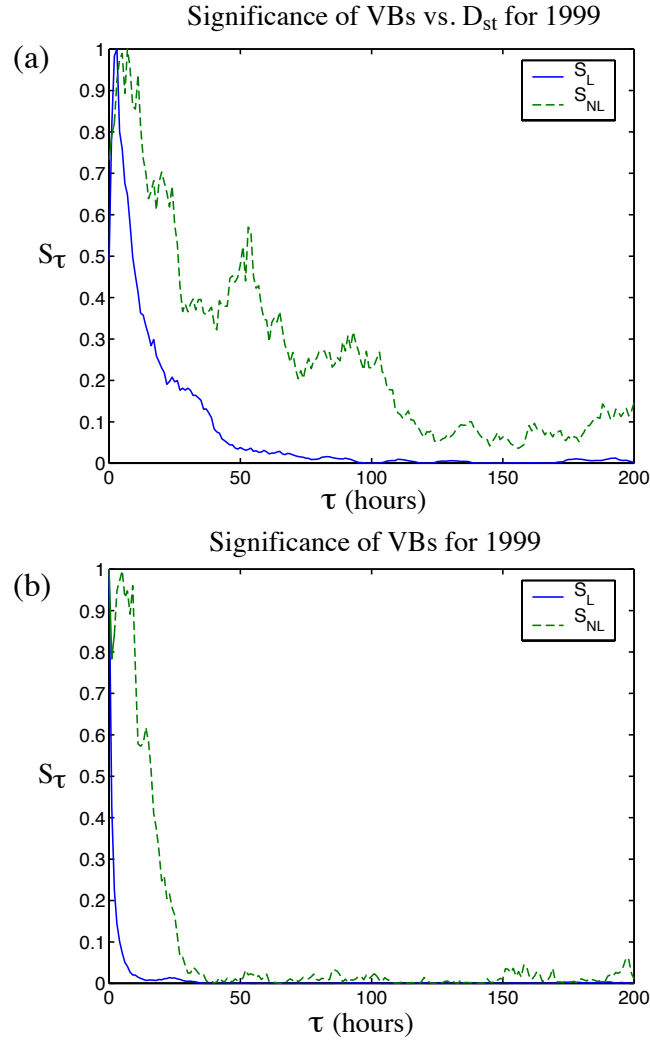


Figure 1. Significance extracted from (a) $\{VBs(t), D_{st}(t-\tau)\}$ and (b) $\{VBs(t), VBs(t-\tau)\}$ for 1999. It should be noted that there is a strong linear response at around 3 hour time delay. There is a clear nonlinear response with a strong peak around 50 hours lasting for approximately 1 week. The longterm nonlinear response is absent in the solar wind data indicating that the longterm nonlinear correlations between VBs and D_{st} are the result of internal magnetospheric dynamics.

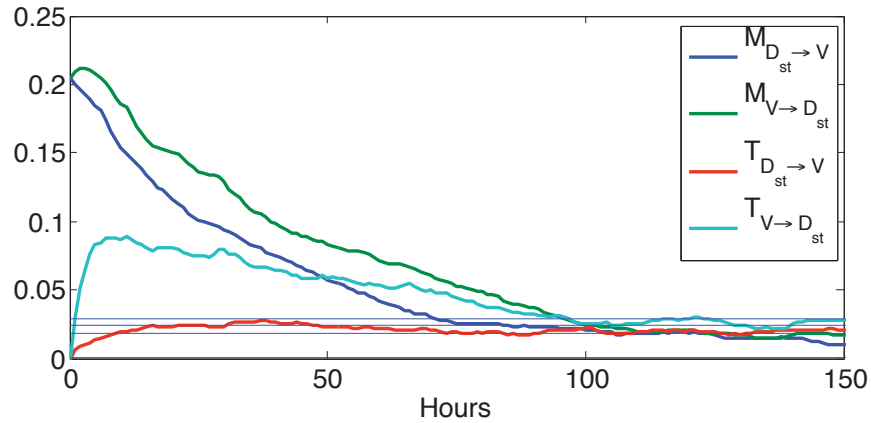


Figure 2. Comparison of mutual information and transfer entropy measures to determine causal driving of the magnetosphere as characterized by D_{st} . Note that causal driving appears to peak somewhat later (11 hours) than indicated by mutual information (2 hours) indicating that internal dynamics likely are very important initially. The backward transfer entropy is below the noise level for all values indicating that D_{st} in no way influences the upstream solar wind velocity. Such a conclusion could not be inferred from the mutual information measure.